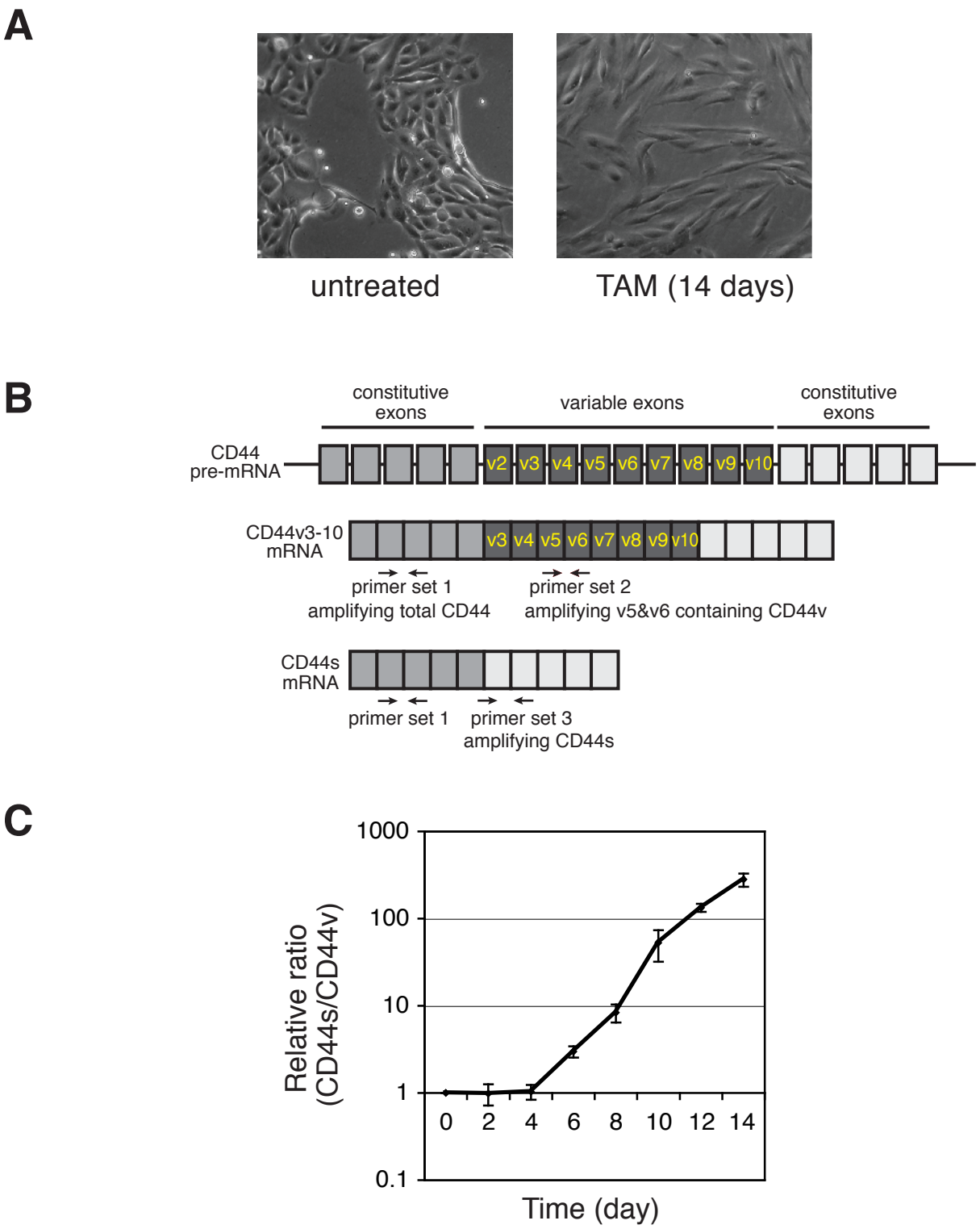

Figure S1. CD44 isoform switching in a Twist-induced EMT model. **A**. Morphological changes during EMT in HMLE/Twist-ER cells after 14 days of tamoxifen (TAM) treatment. Phase contrast images (10X) are shown. **B**. A schematic diagram indicating the locations of primers that are used to measure transcripts of total CD44 (primer set 1), CD44v5/v6 (primer set 2), and CD44s (primer set 3). Note that the forward primer of CD44s spans the exon junction that would otherwise be distroyed by insertion of any variable exons. **C**, qRT-PCR analysis of levels of CD44 isoforms using primers that specifically detect either CD44s (primer set 3 in panel B) or CD44v that contain variable exons v5 and v6 (v5/6, primer set 2). Relative ratios of CD44s to CD44v were normalized to untreated cells at each time points, and results are shown relative to day 0. Error bars indicate s.d., n = 4.

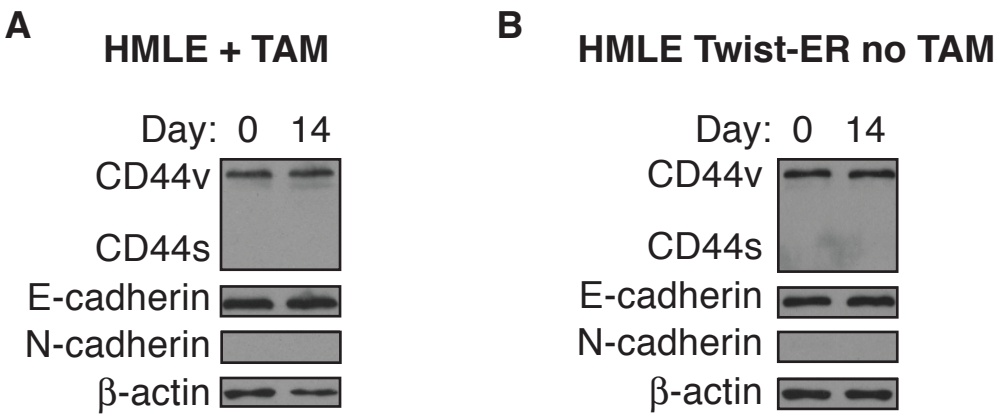

Figure S2. Treatment of HMLE cells with Tamoxifen (TAM) or culturing of HMLE Twist-ER cells in the absence of TAM does not induce a CD44 isoform switch or EMT. **A.** Western blot analysis of parental HMLE cells cultured for 14 days in the presence of TAM. **B.** Western blot analysis of HMLE Twist-ER cells cultured for 14 days in the absence of TAM. Neither of these conditions results in a switch in CD44 isoform expression as shown by the maintainence of CD44v at day 14. Under both conditions, EMT fails to occur as demonstrated by maintained expression of epithelial marker E-cadherin and lack of mesenchymal marker N-cadherin by day 14.

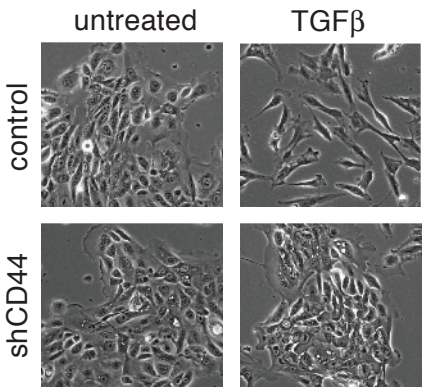

Figure S3. Phase contrast images of HMLE cells expressing a control shRNA or CD44 shRNA (shCD44) before (untreated, left side) and after 18 days of TGFβ treatment (right side). Cells in which CD44 is silenced maintain an epithelial morphology while control cells transition to a mesenchymal phenotype.

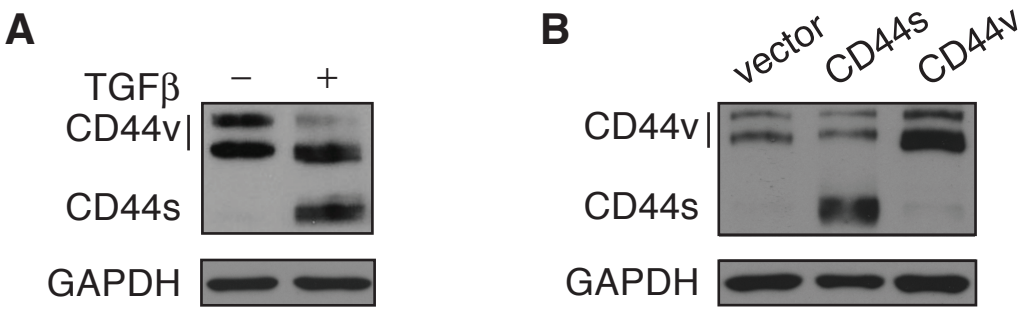

Figure S4. A. Immunoblot analysis showing expression of CD44 isoforms in untreated or TGFβ-treated MCF10A cells demonstrates that treatment with TGFβ results in an increase in CD44s expression. **B.** Immunoblot depicting efficient overexpression of CD44s or CD44v in MCF10A cells.

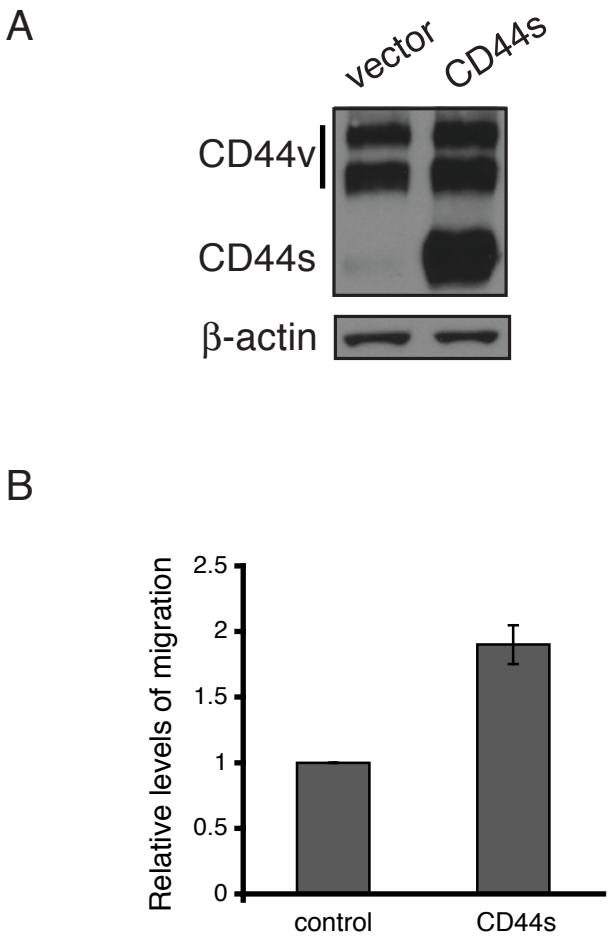

Figure S5. Overexpression of CD44s enhances cell migration. **A.** Immunoblot analysis was performed to show overexpression of a human CD44s construct in MDCK cells as compared to empty vector control cells. **B.** MDCK cells that overexpress CD44s or empty vector control were assayed for migratory ability in transwell migration chambers. Cells at approximately 50% confluency were trypsinized and resuspended in serum free media. Transwell migration chambers (BD) were placed into wells of 24-well tissue culture plates with 750 µl of growth media (10% FBS) as chemoattractant below the chambers. 2 x 10^4 cells were seeded on the top portion of the chamber in a total volume of 500 µl of serum-free media, and the plates were incubated at 37°C for 16-18 hours. Cells that remained on top of the transwell membranes were removed using a cotton swab. Cells that had migrated to the bottom sides of the membranes were fixed in 4% formaldehyde for 10 minutes, stained with crystal violet, and quantified. All conditions were performed in triplicate in each experiment. Results show fold change in migration relative to control for five independent experiments. Error bars represent sem.

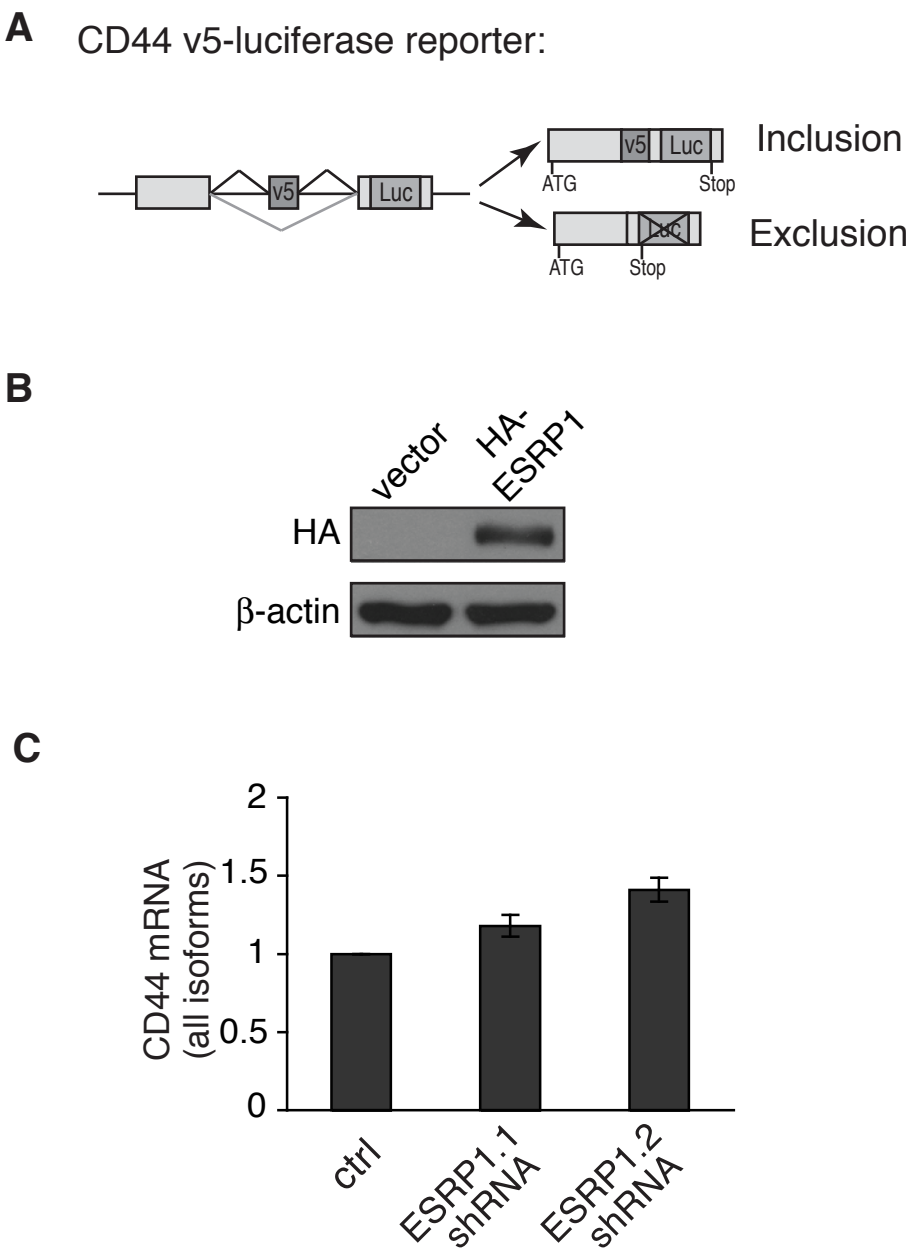

Figure S6. A. Schematic of the CD44v5 mini gene contruct. Inclusion of the v5 exon in the final transcript leads to expression of luciferase, which can be quantified to provide a direct measure of CD44 alternative splicing. Exclusion of v5 prevents luciferase activity by generation of a premature stop codon upstream of luciferase. **B.** Immunoblot analysis showing overexpression of HA-tagged ESRP1 in 293 cells used for luciferase assays. **C.** qRT-PCR analysis of CD44 mRNA using a primer pair that detects all forms of CD44 shows that overall transcription of CD44 does not change when ESRP1 is silenced in HMLE cells. Error bars indicate s.e.m., n = 3.

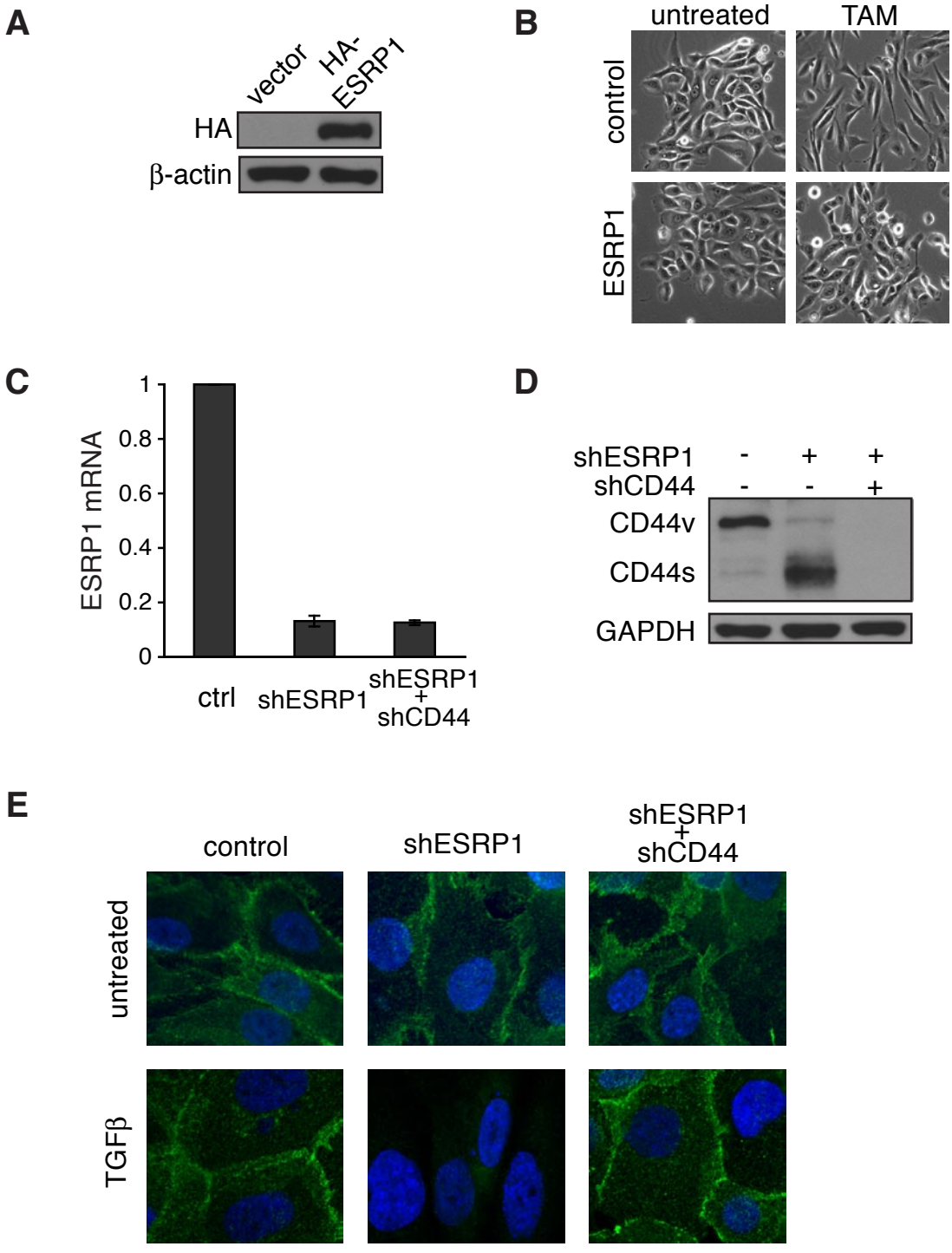

Figure S7. **A.** Immunoblot showing efficient overexpression of HA-tagged ESRP1 in HMLE/Twist-ER cells. **B.** Phase contrast images of HMLE/Twist-ER control or ESRP1-overexpressing cells at day 0 (untreated) or after 14 days of TAM treatment show that cells in which ESRP1 is overexpressed maintain an epithelial morphology while control cells transition to a fibroblastic morphology. **C.** qRT-PCR analysis of ESRP1 in HMLE cells that express ESRP1 shRNA alone or in combination with CD44 shRNA. Error bar represents s.d., n = 3. **D.** Immunoblot showing expression of CD44 isoforms in HMLE cells expressing ESRP1 shRNA alone (middle lane) or in combination with CD44 shRNA (right lane). **E.** Immuno-fluorescence imaging shows that knockdown of ESRP1 results in the accelerated disappearance of E-cadherin at cell junctions as compared to control shRNA-expressing cells in response to TGFβ treatment, but that when CD44 is silenced in the ESRP1-depleted cells, E-cadherin expression is preserved at cell junctions following treatment of TGFβ.

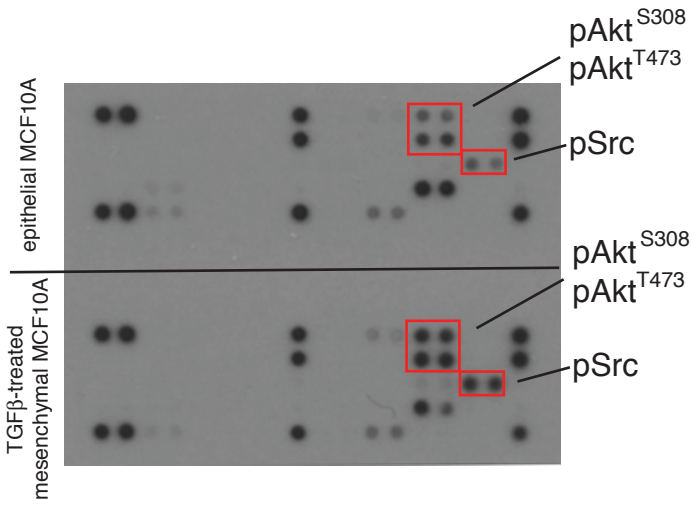

Figure S8. Phospho-protein array showing increased Akt activity in mesenchymal MCF10A cells. Epithelial MCF10A cells or TGFβ-treated mesenchymal MCF10A cells were starved for 24 hours and then stimulated with insulin (1µg/ml) for 30 minutes prior to performing the assay, using the PathScan® RTK Signaling Antibody Array Kit (Cell Signaling Technology, Inc.). Spots representing phosphorylated Akt and Src are highlighted in red boxes. Akt phosphorylation at residues S308 and T473 is increased in the mesenchymal cells by 3.3- and 2.1-fold, respectively. Src phosphorylation is increased by 3.0-fold in the mesenchymal cells.

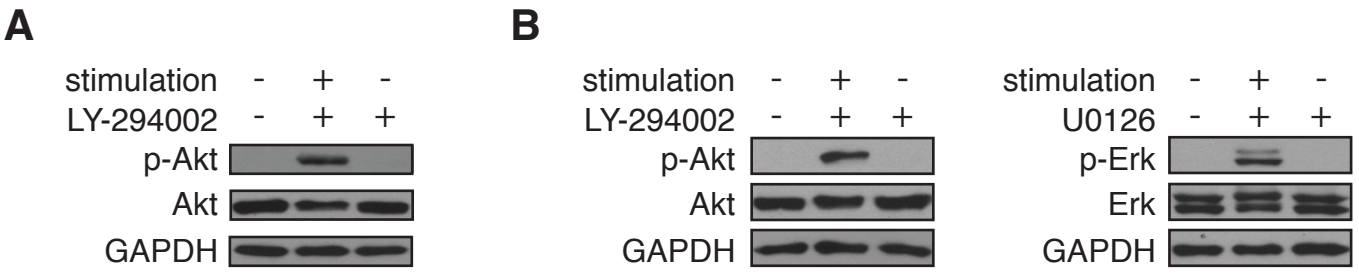

Figure S9. A. Western blot showing levels of phosphorylated Akt (p-Akt) in mesenchymal TGFβ-treated MCF10A cells. Akt is activated upon stimulation with growth media, and this activation is abrogated by treatment with the PI3K inhibitor LY-294002 (50 μM). **B.** Immunoblot demonstrating positive activities of the PI3K inhibitor LY-294002 (50 μM, left) and the MEK inhibitor U0126 (20 μM, right) in TGFβ-treated MCF10A cells that overexpress CD44s.

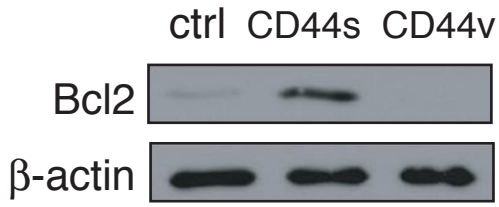

Figure S10. Immunoblot analysis of Bcl2 in TGFβ-treated MCF10A cells expressing vector (ctrl), CD44s, or CD44v, showing that the Bcl2 protein level is upregulated in cells expressing CD44s.

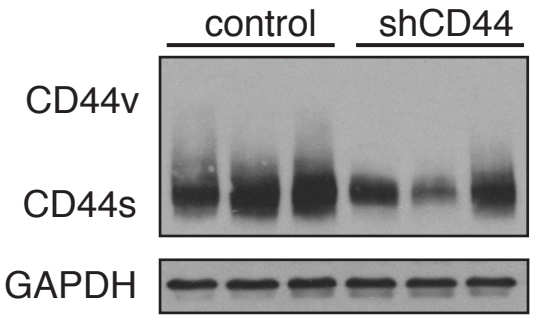

Figure S11. CD44s is re-expressed in tumors derived from CD44 shRNA-expressing cells. Immunoblot analysis of CD44 in recurrent cell line-derived tumors. Note that all of the tumors derived from the shCD44 cell line re-express CD44s, but not CD44v, in vivo.

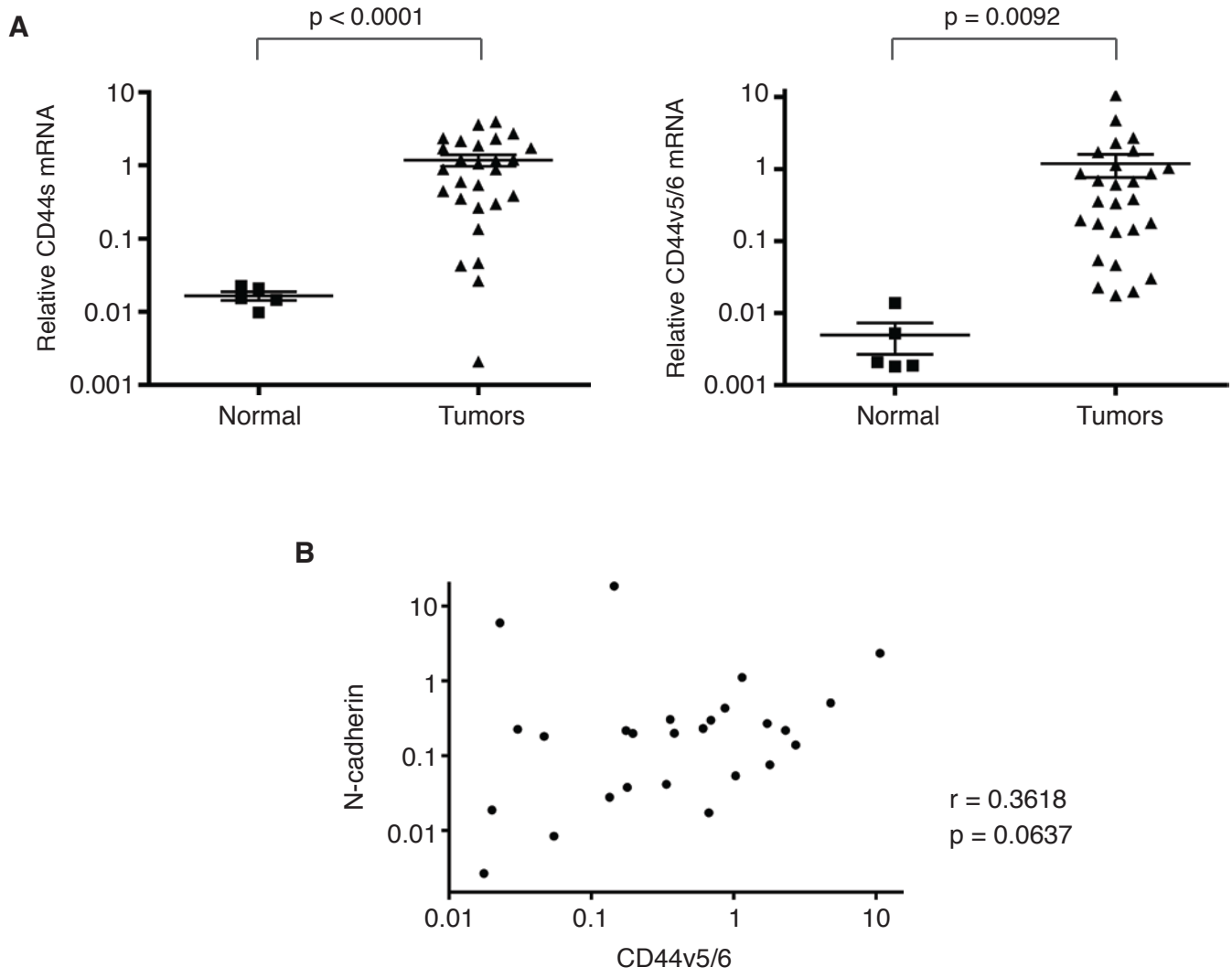

Figure S12. A. qRT-PCR analysis of CD44s (left) and CD44v5/6 (right) mRNA reveals that both CD44s and CD44v are increased in tumors relative to normal tissues. **B.** Relative level of CD44v5/6 in each tumor was plotted against the corresponding N-cadherin level. Spearman correlation analysis revealed no significant association between CD44v and N-cadherin in human tumor samples (Spearman coefficient, r = 0.3618, p = 0.0637).